Research Article

Jinhui Huang, Xue Lin, Yongchuang Zhu, Xuejiao Sun, Jiesheng Chen, and Yingde Cui*

Synthesis and stability of phospholipid-encapsulated nano-selenium

https://doi.org/10.1515/gps-2022-8100
received August 26, 2022; accepted January 11, 2023

Abstract: Red elemental nano-selenium, which is an important biological form of selenium, exhibits very low toxicity and remarkable biological properties and thus has several positive effects. For instance, it shows antioxidation and antistress characteristics, promotes growth and improves immunity. However, owing to its nanoscale size, it is very difficult to disperse and stabilize during synthesis and storage. In this study, nanoscale selenium with a mass content of 2.06% and an average particle size of 49 nm was prepared by the chemical reduction method. The analysis demonstrated that the surface phospholipids formed lamellar structures after directional freezing, and the nano-selenium particles were distributed in the middle of the lamellar. The nano-selenium particles were efficiently dispersed due to their lamellar structure and amphiphilicity. The particles displayed excellent stability and remained relatively unchanged after 20 days of storage in solution or solid state. The difficulties associated with the dispersion and storage stability of nanometer selenium during preparation were solved.

Keywords: nanoscale selenium, SEM imaging, UV-Vis absorbance, stability, nanoparticle aggregation

1 Introduction

Selenium is an essential trace element for animal growth and is an important part of selenoproteins. Selenium deficiency may lead to immune deficiency, muscular dystrophy and exudative inflammation. Different forms of selenium exhibit different functions, including antioxidant ability, promoting cell growth, improving immunity, resisting heat stress, improving intestinal health and regulating body metabolism. Thus, the different forms can be used as selenium supplements for animals [1,2].

In the animal diet, selenium mainly exists in the form of inorganic selenium (selenate and selenite), organic selenium (yeast selenium, selenomethionine and selenocysteine) and nano-selenium (selenium in a simple form). The different forms of selenium are absorbed by animals with different efficiencies through different mechanisms. Under normal physiological conditions, the absorption rate of organic selenium is 70–90%, while the direct absorption rate of selenite is lower than 60%. Because of its small particle size and large specific surface area, nano-selenium can interact with the physiological system rapidly and better maintain the morphology of the intestinal mucosa than yeast selenium. Specifically, it can increase intestinal mucosal permeability and improve intestinal absorption efficiency by forming nano-emulsion droplets. Thus, nano-selenium is used in animal feed because of its high bioavailability and low toxicity [3].

At present, the methods available for synthesizing nano-selenium primarily include chemical and biological routes [4]. The biological methods involve the use of substances produced during microbial growth (such as metabolites and enzymes) as well as plant extracts (such as proteins, flavonoids and vitamins) to reduce selenium salts (sodium selenite and selenite, among others) for synthesizing red nano-selenium particles [5,6]. However, microbial culture and plant extracts require specialized equipment to prepare, involve complex processes that are not environmentally friendly and are present in low contents [7]. Moreover, their presence in higher contents can cause toxicity in the microorganisms themselves. Thus, scaling their production from the laboratory scale to the industrial scale is a major challenge.

The chemical methods involve directly synthesizing nano-selenium by reducing a selenium salt (sodium selenite or selenite) using a reducing agent [8,9]. Generally, a

* **Corresponding author: Yingde Cui,** Guangzhou Vocational College of Science and Technology, Guangzhou 510550, China, e-mail: 13602880087@139.com, tel: +86-20-87411788
Jinhui Huang, Yongchuang Zhu, Xuejiao Sun, Jiesheng Chen: School of Chemical Engineering and Technology, Guangdong Industry Polytechnic, Guangzhou 510330, China; Guangdong Engineering Technical Research Center for Green Household Chemicals, Guangzhou 510330, China
Xue Lin: Guangzhou Tanke Bio-Tech Co., Ltd, Guangzhou 510896, China

surfactant or stabilizer is added during the synthesis process to ensure that the size of the synthesized nano-selenium particles is 0–1,000 nm so that they can exist stably without forming aggregates [10]. However, this requires a high degree of dispersion and can result in instability during long-term storage, resulting in their agglomeration. Thus, most chemical methods use large amounts of dispersants in concentrations of up to 1% [11]. However, dispersants and stabilizers are not conducive to matrix absorption and cause environmental pollution. This limits the use of chemical methods for the large-scale production of nano-selenium in high concentrations.

For example, Blinov et al. [10] prepared nano-selenium by using quaternary ammonium salt for dispersion and vitamin C for reduction. The electrostatic action of quaternary ammonium salt was used to disperse nano-selenium. However, due to the low selenic acid dispersion concentration (0.036 mol·L^{-1}), only the solution state was studied. Salem et al. [12] used orange peel waste for selenium nanoparticles with a concentration of 2 mM Na_2SeO_3. This concentration was extremely low and only the solution state was investigated.

Therefore, red nano-selenium particles were synthesized using sodium selenite as the selenium source, vitamin C as the reducing agent, soybean phospholipid and water-soluble starch as the stable dispersant. In addition to the solution state, the storage stability was investigated. Because of their unique molecular structure, phospholipids readily form molecular layers [13,14]. Thus, we attempted to disperse and encapsulate the nano-selenium particles between two films of phospholipids by directional freezing to prevent their agglomeration and ensure their stability and synthesis in a high concentration. Moreover, this method uses a phospholipid and water-soluble starch as stabilizers. Both exhibit good biocompatibility and thus do not prevent matrix absorption, in contrast to surfactants.

2 Materials and methods

2.1 Synthesis of nano-selenium

As shown in Figure 1, 13.5 g of water-soluble starch was added to 180 mL of deionized water, and the mixture was heated to 90°C. Next, the temperature was reduced to 50°C, and 4.0 g of a soybean phospholipid (Beijing Chinaholder Biotech Co., Ltd) was added to the solution under magnetic stirring. Subsequently, 0.9 g of sodium selenite was dissolved in the solution. The solution

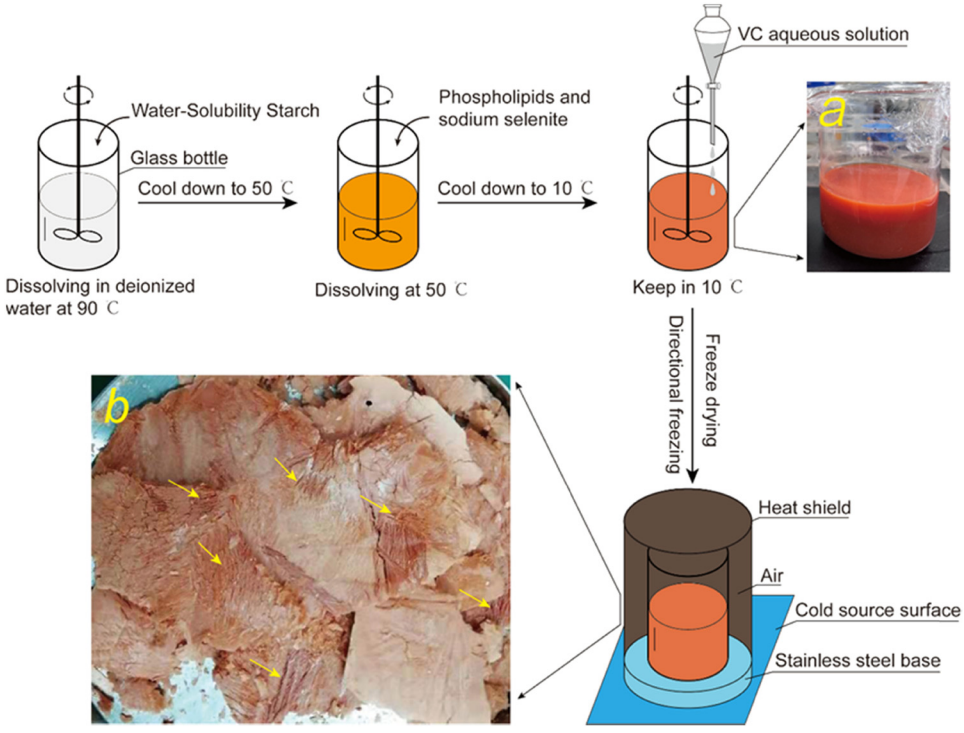

Figure 1: Synthesis of nano-selenium: (a) digital picture of synthesized solution sample and (b) digital picture of freeze-dried sample.

temperature was reduced to 10°C and 20 mL of a vitamin C (VC) solution (0.1 g·mL^{-1}) was slowly added. The reaction proceeded for 1 h to obtain a nano-selenium suspension, as shown in Figure 1a. Finally, directional freezing was performed followed by freeze-drying to obtain the desired product, as shown in Figure 1a. The yellow arrows in the figure point to the layers or sheets of the final product.

2.2 Determination of nano-selenium concentration

To determine the concentration of nano-selenium in the obtained product, 0.1000 g of the product was weighed and digested using nitric acid and perchloric acid. The solution was then diluted with 50% hydrochloric acid to the corresponding concentration. Next, the solution was analyzed using a dual-channel atomic fluorescence spectrometer, and the selenium content was determined using the expression given below:

$$\text{Selenium content (\%)} = \frac{c \times V \times N}{m \times 10^4} \quad (1)$$

where c is the concentration of nano-selenium in the test solution (ng·mL^{-1}), V is the volume of the test solution (mL), N is the dilution multiple of the test solution and m is the quantity of the sample to be weighed (g).

2.3 Structural characterization and performance evaluation

A scanning electron microscopy (SEM) system (EVO 18, Carl Zeiss, Jena, Germany) was used to evaluate the particle size, morphology and distribution of the nano-selenium particles in the obtained sample. Energy-dispersive X-ray spectroscopy (EDS, EVO18) was used to analyze the elemental distribution of the sample. An ultraviolet–visible (UV-Vis) absorption spectrophotometer (Lambda 25, PerkinElmer, America) was also used to characterize the nano-selenium particles. The analysis was performed for the wavelength range of 200–500 nm. Finally, a dual-channel atomic fluid spectrometer (AFS-2000, Beijing Kechuang Haiguang Instrument Factory) was used to determine the concentration of selenium in the obtained sample. X-ray diffraction (XRD) patterns were measured using a D8 Advance (Brucker, Germany) diffractometer (Cu Kα radiation) at a generator voltage of 40 kV. The thermal performance of our samples was analyzed using a differential scanning calorimeter (DSC, Q2000, TA Instruments, New Castle, DE, USA) at a scanning rate of 10°C·min^{-1}. Thermogravimetric analysis (TGA) curves were obtained with a TGA2 (Mettler Toledo, Columbus, OH, USA) at a heating rate of 10°C·min^{-1} in a nitrogen atmosphere.

3 Results and discussion

After freezing the nano-selenium-containing solution shown in Figure 1a and thawing it to room temperature, a flaky solid was obtained, as shown in Figure 2a. Subsequently, after freeze-drying, the flaky material shown in the yellow box in Figure 2b was obtained. SEM analysis showed that the material is lamellar (Figure 2c), with a large number of nano-selenium particles attached to the sheets (Figure 2d). Generally, the nanoparticles are coated with phospholipids to form a microcapsule. And in this study, the synthesized nanoparticles exhibited homogenous morphologies. However, during directed freezing, the phospholipids in the solution interact with and realign along the surface of the ice crystals, resulting in the development of lamellar phospholipids, due to the frame-induced effect [15]. The average particle size was approximately 49 nm, as determined using the software ImageJ. Thus, it was confirmed that nano-selenium particles were synthesized successfully using the proposed method. Moreover, the use of the phospholipid resulted in the formation of a lamellar structure after directional freezing, with the nano-selenium particles dispersed within these lamellar structures.

The samples were characterized by DSC, TGA and XRD (Figure 3). There were no obvious crystal spectral features according to XRD (Figure 3a). This indicates that the prepared nano-selenium was amorphous, containing only nano-selenium aggregates. As can be seen from Figure 3b, when the sample exceeds 250°C, it began to dissolve slowly, indicating that when the sample was below 250°C, there was no other substance except partial evaporation of water. The DSC analysis exhibits two heat-absorbing peaks near 56.7°C and 229.7°C, which are, respectively, attributed to the melting temperatures of a-Se and t-Se (Figure 3c) [16]. The exothermic peak appeared at 112.3°C, indicating that the crystallinity of a-Se in the melting state increased, changing the crystal type to tripartite t-Se.

The selenium concentration of the sample was determined using the method described in Section 2.2 and found to be 2.06 wt%. To analyze the distribution of the nano-selenium particles within the lamellae, EDS analysis was performed. After freeze-drying, lamellae were

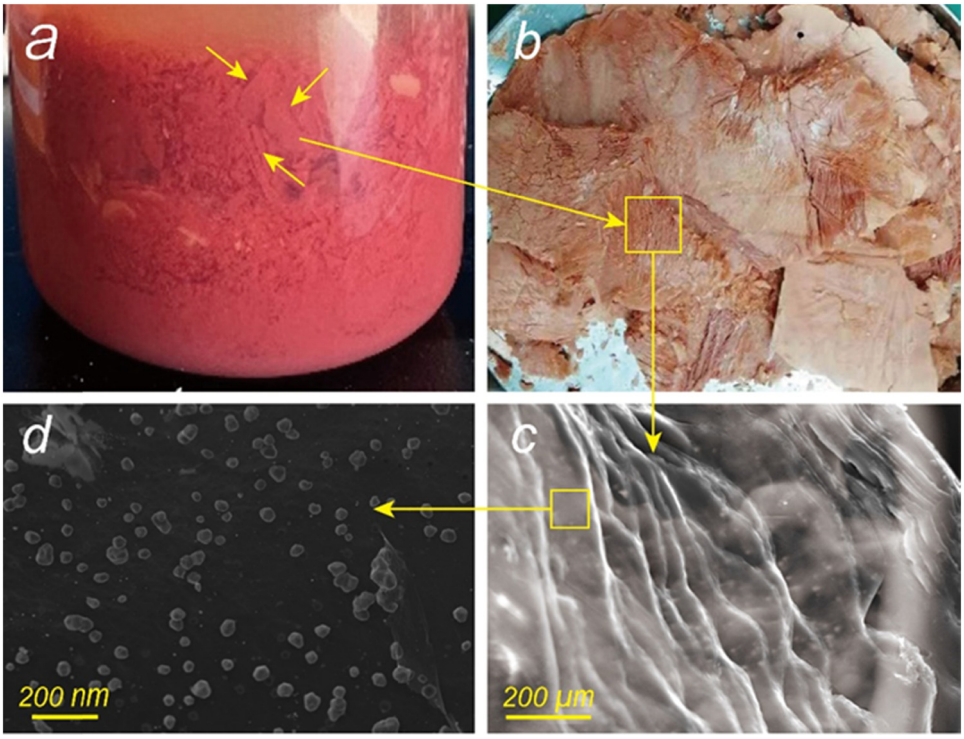

Figure 2: Digital and electron microscopy images of the synthesized sample: (a) digital pictures after freeze-thawing, (b) digital pictures of samples after freeze-drying and (c and d) electron microscopic images after freeze-drying.

formed due to the frame-induced effect of ice crystals, and nano-selenium particles were randomly distributed on the lamellae (Figure 4a and b). During directional freezing, the excess phospholipids in the solution formed the lamellar layer while the phospholipids remained wrapped on the nano-selenium, preventing aggregation. The mass content of selenium was determined as 2.35% via EDS (Figure 4c), which was consistent with the detected concentration. The selenium nanoparticles were subjected to another round of directional freeze drying and were found to be evenly and randomly distributed.

Next, to evaluate the particle size and stability of the nano-selenium particles sandwiched within the phospholipid lamellae, UV-Vis absorption spectrophotometry was performed. According to the literature [17–19], an increase in the size of nano-selenium particles increases the UV absorption wavelength of the suspension. As per previous reports, the average diameter corresponding to the absorption peaks observed at wavelengths smaller than 300 nm is less than 70.9 ± 9.1 nm (Figure 5). This is consistent with the results of this study, wherein the adsorption peak wavelength was determined to be

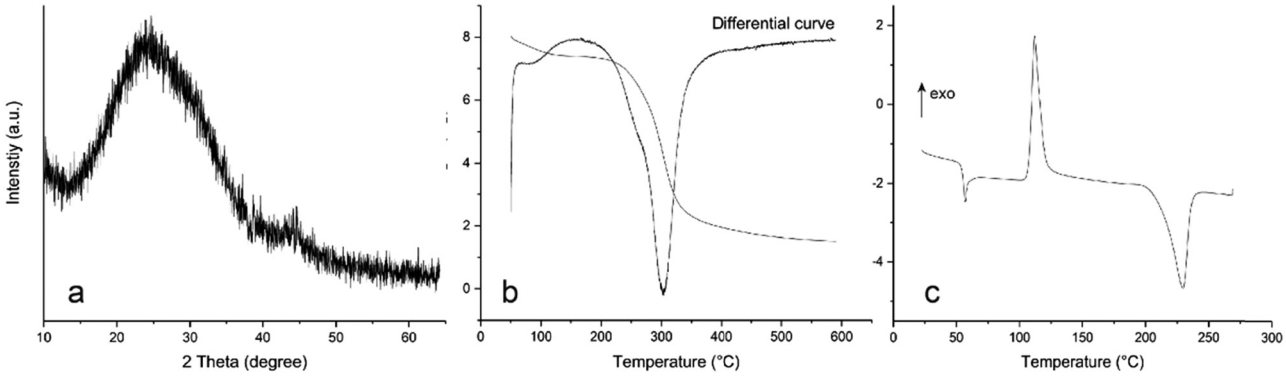

Figure 3: XRD, TGA and DSC spectrogram of the sample: (a) XRD curve, (b) TGA curve and (c) DSC curve.

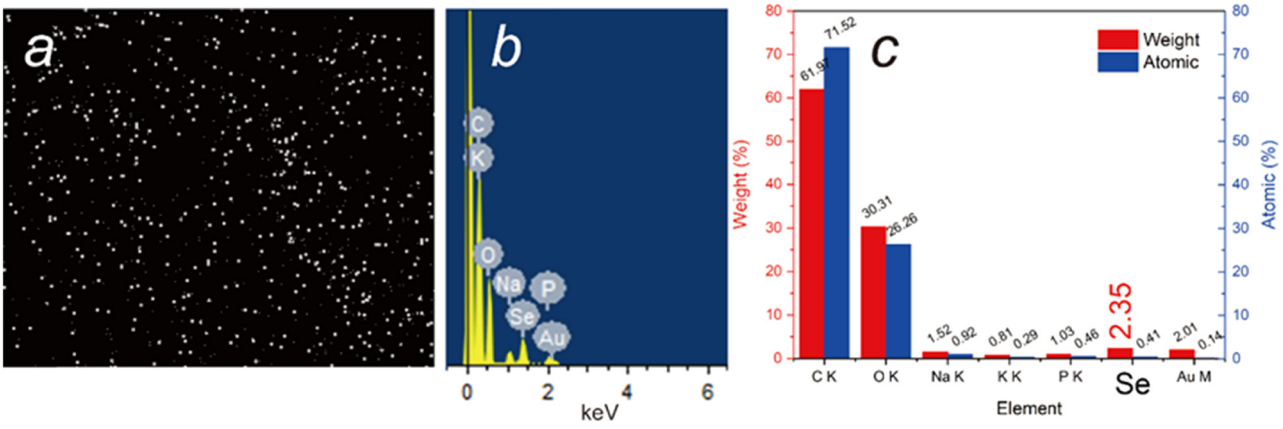

Figure 4: EDS spectrum of synthesized sample and results of its elemental analysis: (a) distribution spectrum of selenium in the sample, (b) energy spectra of each element contained in the sample and (c) content of each element in the sample.

264 nm and the average size of the nano-selenium particles was 49 nm. At the same time, the stability of the sample was also verified. A newly prepared liquid sample not subjected to freeze drying, a sample subjected to freeze drying and a sample stored for 20 days after freeze drying were subjected to UV-Vis absorption spectrophotometry. The results are shown in Figure 5. It can be seen that the absorption peak did not move significantly, indicating that the nano-selenium particles did not undergo significant aggregation during the freeze drying and storage processes and thus exhibited good stability. The stability of the nano-selenium particles in the liquid state was also investigated. It can be seen from Figure 5 that the absorption peak of the nano-selenium particles in a non-lyophilized solution shifted to a higher wavelength after storage for 10 and 20 days. However, the shift was not pronounced, indicating that while the nano-selenium particles formed some aggregates, their absorption peak wavelength remained lower than 300 nm even after 20 days. Thus, the average particle size remained smaller than 70 nm, indicating that the nano-selenium particles were stable even in a solution.

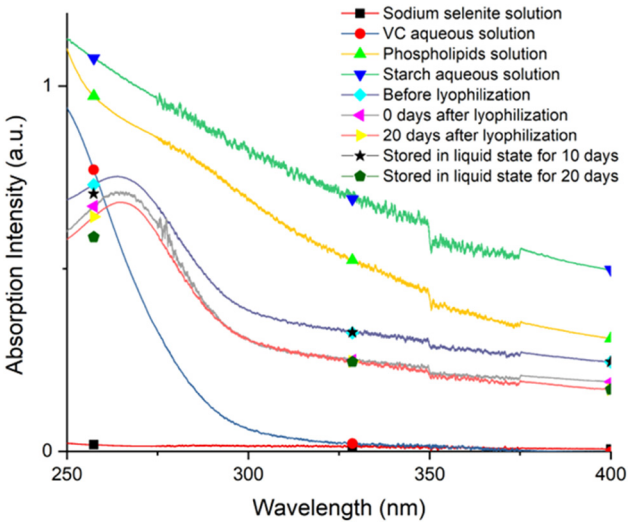

Figure 5: UV absorption curves of various solutions.

4 Conclusions

In this study, inorganic selenium was reduced by VC and dispersed using a phospholipid to obtain a suspension of nano-selenium particles with a concentration of approximately 2.06% and an average particle size of approximately 49 nm. Because of the unique molecular structure of the phospholipid, it readily formed a molecular layer, which transformed into a lamellar structure after directional freeze drying. SEM imaging confirmed that the nano-selenium particles formed an interlayer within the lamellar structure of the phospholipid. UV-Vis absorption analysis confirmed that the nano-selenium particles did not form aggregates for up to 20 days both in solid and solution forms and thus exhibited high stability. In comparison to earlier research, this study was characterized by simple preparation and high stability. The dispersed system utilized eco-friendly bio-derived raw ingredients. Importantly, the concentration of nano-selenium synthesized by this methodology was relatively high, approaching industrial production levels, and had a wide range of applications.

Acknowledgment: This work was supported by Guangzhou Tanke Bio-Tech Co., Ltd, in samples testing.

Funding information: This study was supported by the Research Project of Guangdong Industry Polytechnic (KJ2021-08).

Author contributions: Jinhui Huang: conceptualization, investigation, methodology, writing – original draft; Xue Lin: resources; writing – review and editing; Yongchuang Zhu: writing – review and editing; Xuejiao Sun: formal analysis; Jiesheng Chen: visualization; Yingde Cui: project administration, funding acquisition.

Conflict of interest: Authors state no conflict of interest.

References

[1] Kumar A, Prasad KS. Role of nano-selenium in health and environment. J Biotechnol. 2021;325(4):152–63. doi: 10.1016/j.jbiotec.2020.11.004.

[2] Farah SD, Emad K, Ali H. Synthesis Of selenium nanoparticles. Eurasian J Phys Chem Math. 2022;7(3):67–71. doi: 10.1038/s41598-019-57333-7.

[3] Bhattacharjee A, Basu A, Bhattacharya S. Selenium nanoparticles are less toxic than inorganic and organic selenium to mice in vivo. Nucleus. 2019;62(3):259–68. doi: 10.1007/s13237-019-00303-1.

[4] Khanna PK, Bisht N, Phalswal P. Selenium nanoparticles: A review on synthesis and biomedical applications. Mater Adv. 2022;3(1):1415–31. doi: 10.1039/D1MA00639H.

[5] Cui YH, Li LL, Zhou NQ, Liu JH, Huang Q, Wang HJ, et al. In vivo synthesis of nano-selenium by Tetrahymena thermophila SB210. Enzyme Microb Technol. 2016;95(5):185–91. doi: 10.1016/j.enzmictec.2016.08.017.

[6] Akcay FA, Avci A. Effects of process conditions and yeast extract on the synthesis of selenium nanoparticles by a novel indigenous isolate Bacillus sp. EKT1 and characterization of nanoparticles. Arch Microbiol. 2020;202(8):2233–43. doi: 10.1007/s00203-020-01942-8.

[7] Hashem AH, Khalil AMA, Reyad AM, Salem SS. Biomedical applications of mycosynthesized selenium nanoparticles using penicillium expansum ATTC 36200. Biol Trace Elem Res. 2021;199(10):3998–4008. doi: 10.1007/s12011-020-02506-z.

[8] Yunusov KE, Sarymsakov AA, Turakulov FM. Synthesis and physicochemical properties of the nanocomposites based on sodium carboxymethyl cellulose and selenium nanoparticles. Polym Sci Ser B. 2022;64(1):68–77. doi: 10.1134/s1560090422010080.

[9] Alam H, Khatoon N, Raza M, Ghosh PC, Sardar M. Synthesis and characterization of nano selenium using plant biomolecules and their potential applications. BioNanoScience. 2018;9(1):96–104. doi: 10.1007/s12668-018-0569-5.

[10] Blinov AV, Maglakelidze DG, Yasnaya MA, Gvozdenko AA, Blinova AA, Golik AB, et al. Synthesis of selenium nanoparticles stabilized by quaternary ammonium compounds. Russ J Gen Chem. 2022;92(3):424–9. doi: 10.1134/s1070363222030094.

[11] Wen S, Hui Y, Chuang W. Biosynthesis and antioxidation of nano-selenium using lemon juice as a reducing agent. Green Process Synth. 2021;10(1):178–88. doi: 10.1515/gps-2021-0018.

[12] Salem SS, Badawy MSEM, Al-Askar AA, Arishi AA, Elkady FM, Hashem AH. Green biosynthesis of selenium nanoparticles using orange peel waste: Characterization, antibacterial and antibiofilm activities against multidrug-resistant bacteria. Life. 2022;12(6):893.

[13] Sut TN, Park S, Yoon BK, Jackman JA, Cho NJ. Supported lipid bilayer formation from phospholipid-fatty acid bicellar mixtures. Langmuir. 2020;36(18):5021–9. doi: 10.1021/acs.langmuir.0c00675.

[14] Jackman JA, Cho NJ. Supported lipid bilayer formation: Beyond vesicle fusion. Langmuir. 2020;36(6):1387–400. doi: 10.1021/acs.langmuir.9b03706.

[15] Dong Y, Sun Y, Wang L, Wang D, Zhou T, Yang Z, et al. Frame-guided assembly of vesicles with programmed geometry and dimensions. Angew Chem Int Ed. 2014;53(10):2607–10. doi: 10.1002/anie.201310715.

[16] Chen Z, Shen Y, Xie A, Zhu J, Wu Z, Huang F. L-cysteine-assisted controlled synthesis of selenium nanospheres and nanorods. Cryst Growth Des. 2009;9(3):1327–33. doi: 10.1021/cg800398b.

[17] Vahdati M, Tohidi Moghadam T. Synthesis and characterization of selenium nanoparticles-lysozyme nanohybrid system with synergistic antibacterial properties. Sci Rep. 2020;10(1):501–10. doi: 10.1038/s41598-019-57333-7.

[18] Lin Z-H, Chris Wang CR. Evidence on the size-dependent absorption spectral evolution of selenium nanoparticles. Mater Chem Phys. 2005;92(2–3):591–4. doi: 10.1016/j.matchemphys.2005.02.023.

[19] Asghari-Paskiabi F, Imani M, Razzaghi-Abyaneh M, Rafii-Tabar H. Fusarium oxysporum, a bio-factory for nano selenium compounds: Synthesis and characterization. Sci Iran. 2018;25(3):1857–63. doi: 10.24200/sci.2018.5301.1192.